

RESEARCH ARTICLE

Maternal DCAF2 is crucial for maintenance of genome stability during the first cell cycle in mice

Yi-Wen Xu¹, Lan-Rui Cao¹, Min Wang², Ying Xu³, Xin Wu², Junping Liu⁴, Chao Tong¹ and Heng-Yu Fan^{1,4,*}

ABSTRACT

Precise regulation of DNA replication and genome integrity is crucial for gametogenesis and early embryogenesis. Cullin ring-finger ubiquitin ligase 4 (CRL4) has multiple functions in the maintenance of germ cell survival, oocyte meiotic maturation, and maternal-zygotic transition in mammals. DDB1–cullin-4-associated factor-2 (DCAF2, also known as DTL or CDT2) is an evolutionarily conserved substrate receptor of CRL4. To determine whether DCAF2 is a key CRL4 substrate adaptor in mammalian oocytes, we generated a novel mouse strain that carries a *Dcaf2* allele flanked by *loxP* sequences, and specifically deleted *Dcaf2* in oocytes. *Dcaf2* knockout in mouse oocytes leads to female infertility. Although *Dcaf2*-null oocytes were able to develop and mature normally, the embryos derived from them were arrested at one- to two-cell stage, owing to prolonged DNA replication and accumulation of massive DNA damage. These results indicate that DCAF2 is a previously unrecognized maternal factor that safeguards zygotic genome stability. Maternal DCAF2 protein is crucial for prevention of DNA re-replication in the first and unique mitotic cell cycle of the zygote.

This article has an associated First Person interview with the first author of the paper.

KEY WORDS: Oocyte, Maternal-zygotic transition, Zygote, Female fertility, DNA replication, CRL4

INTRODUCTION

In mammals, female germ cells exit mitosis after their last round of DNA replication, enter meiosis on embryonic days 11.5–12.5, and are arrested at the diplotene stage of prophase I for an extended period (Smallwood and Kelsey, 2012). Within 3 days of birth, these oocytes are enclosed by ovarian somatic cells for formation of primordial follicles (Zhang and Liu, 2015). DNA replication is halted in these follicle-enclosed oocytes for months in experimental rodents or up to 50 years in humans.

Shortly after fertilization and pronucleus formation, the first round of DNA replication of the embryo is initiated with several distinct features: (1) the DNA replication machinery is assembled by maternal factors stored in the oocyte; (2) DNA replication is initiated and progresses separately in haploid male and female nuclei, respectively; (3) the DNA replication in the zygote is accompanied by drastic

genome remodeling, including massive DNA demethylation, histone modifications and histone replacement (Akiyama et al., 2011; Murai et al., 2014; Swiech et al., 2007; Xu et al., 2015). It has been proposed that genome remodeling after fertilization, particularly in the male nucleus, induces DNA damage including both single- and double-strand breaks (Hajkova et al., 2010; Nakatani et al., 2015). The damaged DNA is repaired in the first round of replication (Ma et al., 2016; Wang et al., 2013). It is unclear whether repair of the genome remodeling-induced DNA damage is a prerequisite for subsequent cleavages, and if so, which maternal factors are necessary for repairing the DNA damage and for maintaining zygotic genome integrity during oocyte-to-embryo transition.

Our studies have shown that cullin ring-finger ubiquitin ligase 4 (CRL4) has multiple functions in the maintenance of oocyte survival, meiotic cell cycle progression, and genome reprogramming after fertilization (Yu et al., 2015a,b, 2013). We and others have also reported that the CRL4 components cullin 4A and DDB1 are essential for spermatogenesis in mice and *Drosophila* (Kopanja et al., 2011; Yu et al., 2016b). CRL4 plays versatile biological roles by employing >90 WD40 repeat-containing adaptor proteins, known as DDB1–cullin-4-associated factors (DCAFs) (Lee and Zhou, 2007). These DCAFs recruit a wide spectrum of substrates to CRL4 for poly- or monoubiquitylation (Bennett et al., 2010). DCAF2, also known as DTL or CDT2, is one of the best-studied substrate receptors of CRL4 (Abbas and Dutta, 2011). For ubiquitin-mediated degradation, DCAF2 targets a number of substrates, such as CDT1, p21 (also known as CDKN1A) and CHK1 (also known as CHEK1), involved in regulation of the cell cycle and survival (Havens and Walter, 2011).

DCAF2 overexpression has been reported in breast (Ueki et al., 2008) and ovarian (Pan et al., 2013) carcinomas and rhabdomyosarcomas (Missiaglia et al., 2009), and contributes to chemotherapy resistance of ovarian cancer cells (Pan et al., 2013). By contrast, the *in vivo* function of DCAF2 in development has been poorly studied. Targeted disruption of the *Dcaf2* gene in mice causes early embryonic mortality (Liu et al., 2007). The zygotic *Dcaf2* knockout embryos (*Dcaf2*^{-/-}) terminate development at the four- to eight-cell stage (Liu et al., 2007). This situation has prevented research into the role of DCAF2 in later developmental processes including gametogenesis. Furthermore, the maternally contributed DCAF2 might compensate for the loss of zygotic DCAF2 in the first two embryonic cell cycles.

To specifically determine whether DCAF2 is one of the key CRL4 substrate adaptors in oogenesis, we generated a novel mouse strain that carries a *Dcaf2* allele flanked by *loxP* sequences, and deleted *Dcaf2* in oocytes using cell type-specifically expressed Cre DNA recombinase. The results showed that the maternal DCAF2 protein is crucial for prevention of DNA re-replication in the first and unique mitotic cell cycle of the zygote. We also report that DCAF2 plays a previously unrecognized role in the regulation of DNA demethylation during oocyte-to-embryo transition in mice.

¹Life Sciences Institute, Zhejiang University, Hangzhou 310058, China. ²State Key Laboratory of Reproductive Medicine, Nanjing Medical University, Nanjing 210029, China. ³Cambridge-Suda Genomic Resource, Soochow University, Suzhou 215123, China. ⁴Institute of Aging Research, Hangzhou Normal University, Hangzhou 311121, China.

*Author for correspondence (hyfan@zju.edu.cn)

 H.-Y.F., 0000-0003-4544-4724

RESULTS

The expression of DCAF2 and its putative targets in oocytes and early embryos

We first examined the expression and distribution of DCAF2 in oocytes. By conducting quantitative real-time PCR, we found that *Dcaf2* mRNA is expressed much more strongly in fully grown oocytes and zygotes than in representative somatic tissues (Fig. 1A). *Dcaf2* expression further increased in two- to eight-cell embryos after major zygotic genome activation, and then decreased in morulae and blastocysts (Fig. 1B). Unfortunately, the available commercial anti-DCAF2 antibodies failed to detect endogenous

DCAF2 in mouse oocytes and zygotes. Therefore, we expressed an mCherry-tagged DCAF2 in oocytes and zygotes by mRNA microinjection followed by fluorescence staining to study its localization. The DCAF2 protein was found to be evenly distributed in germinal vesicle (GV)-stage oocytes, but showed larger amounts in pronuclei than in the zygotic cytoplasm after fertilization (Fig. 1C). The nuclear localization of DCAF2 became more prominent in two- to four-cell embryos (Fig. 1C). Collectively, these results suggested that DCAF2 is highly expressed in mouse oocytes and zygotes, and might be intimately involved in the first mitotic cell cycle progression.

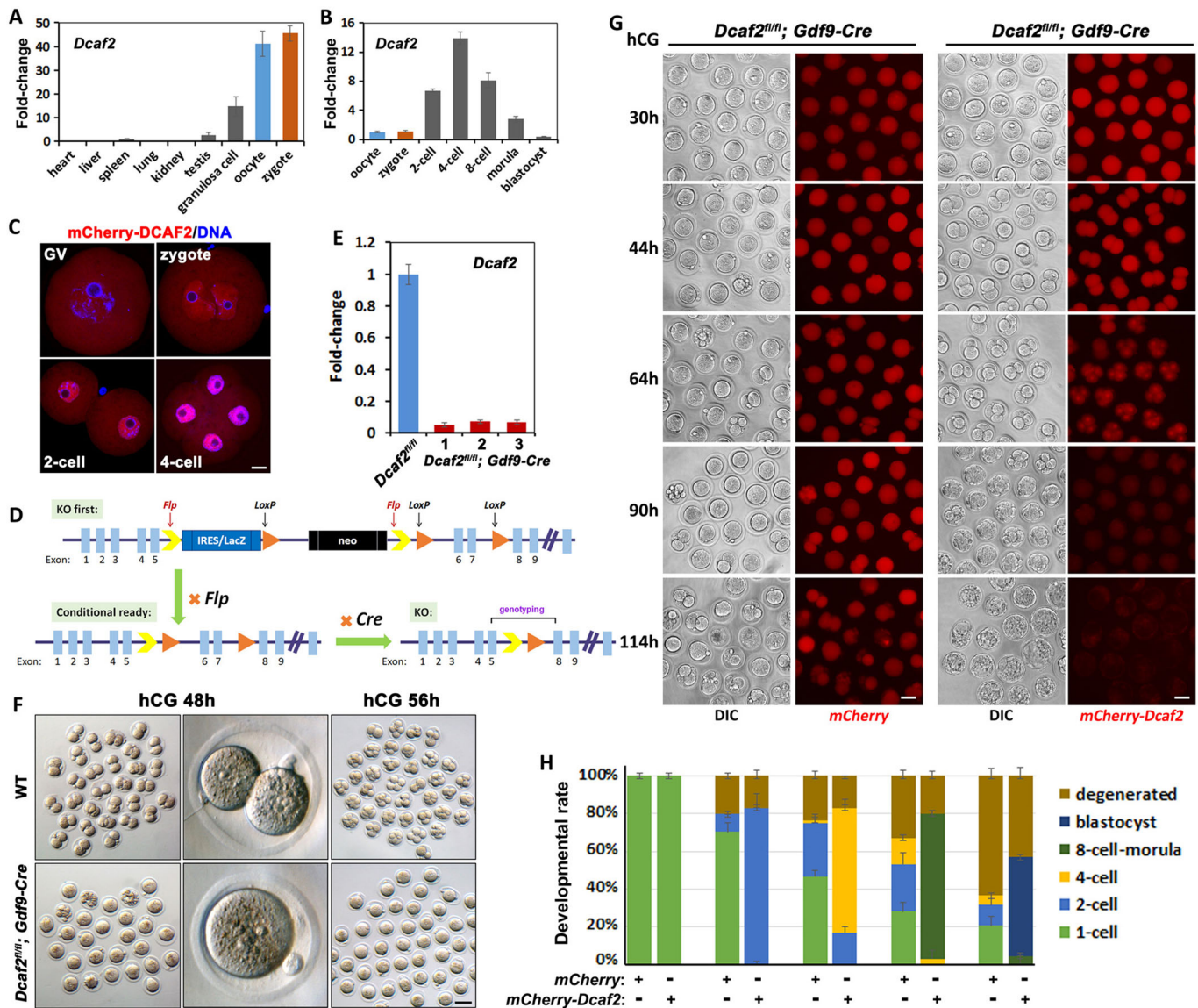


Fig. 1. Expression and conditional knockout of DCAF2 in mouse oocyte and early embryos. (A,B) Real-time RT-PCR results showing relative *Dcaf2* mRNA levels in somatic tissues, oocytes and early embryos. (C) Localization of mCherry-DCAF2 proteins in oocytes and zygotes. Mouse oocytes or zygotes were microinjected with 5–10 pl *mCherry-Dcaf2* mRNA. After microinjection, oocytes were cultured overnight in M16 medium containing 2 μ M milrinone to inhibit spontaneous GVBD, and zygotes were cultured in KSOM. Samples were fixed at the indicated developmental stages for fluorescent microscopy. (D) Schematic of the insertion of *Flp* and *loxP* sequences into the mouse *Dcaf2* gene locus, and the generation of oocyte-specific *Dcaf2* knockout mice. (E) Quantitative RT-PCR results showing *Dcaf2* mRNA levels in fully grown GV oocytes ($n=10$ for each sample) isolated from the ovaries of *Dcaf2*^{fl/fl} and *Dcaf2*^{fl/fl}; *Gdf9-Cre* females, at postnatal day 23. (F) Representative images of embryos flushed from the oviducts of WT and *Dcaf2*^{fl/fl}; *Gdf9-Cre* females at 48 h and 56 h after hCG injection. (G) Expression of exogenous DCAF2 rescued the developmental arrest of *Dcaf2*^{fl/fl}; *Gdf9-Cre* zygotes. mRNAs encoding mCherry (as control) and mCherry-DCAF2 were microinjected into *Dcaf2*^{fl/fl}; *Gdf9-Cre* zygotes and cultured in KSOM *in vitro*. Zygotes injected with mCherry were arrested at one- or two-cell stage, whereas >50% of the zygotes injected with mCherry-DCAF2 developed to blastocyst stage. (H) Quantification of the developmental rates of *Dcaf2*^{fl/fl}; *Gdf9-Cre* zygotes microinjected with mRNAs encoding mCherry or mCherry-DCAF2. $n=64$ for each experimental group. Scale bars: 10 μ m in C; 50 μ m in G; 100 μ m in F.

An oocyte-specific *Dcaf2* knockout causes female infertility

To determine the *in vivo* function of maternal *Dcaf2*, we generated a mouse strain that carries a *Dcaf2* allele flanked by *loxP* sequences (*Dcaf2^{fl/fl}*) (Fig. 1D) and deleted maternal *Dcaf2* using oocyte-specifically expressed *Gdf9-Cre* DNA recombinase (*Dcaf2^{fl/fl}; Gdf9-Cre*). The *Dcaf2* deletion was confirmed by quantitative RT-PCR in oocytes isolated from the ovaries of *Dcaf2^{fl/fl}* and *Dcaf2^{fl/fl}; Gdf9-Cre* females (Fig. 1E). The females were completely infertile when mated with wild-type (WT) males. To identify the reason for the infertility of *Dcaf2^{fl/fl}; Gdf9-Cre* females, we collected embryos from the oviducts of control and mutant females 48 h and 56 h after human chorionic gonadotropin (hCG) injection. While embryos from control females developed to two-cell (hCG 48 h) and four-cell (hCG 56 h) stages, embryos from *Dcaf2^{fl/fl}; Gdf9-Cre* females (later termed *Dcaf2^{♀-/-♂+}*) were all arrested at the zygote stage and contained normal male and female pronuclei (Fig. 1F). These results indicated that maternal *Dcaf2* is required for completion of the first mitotic division of the zygote.

Because DCAF2 deletion in somatic cells causes DNA damage and apoptosis (Kim et al., 2008; Pan et al., 2013), we investigated the potential involvement of DCAF2 in the maintenance of oocyte survival. Ovaries of adult (4 to 6 months old) *Dcaf2^{fl/fl}; Gdf9-Cre* mice are normal histologically (Fig. S1A). Immunohistochemical staining for the oocyte marker mouse vasa homolog (MVH) revealed that oocytes were present in both primordial follicles and in

growing follicles (Fig. S1B). After superovulation, *Dcaf2^{fl/fl}; Gdf9-Cre* females ovulated metaphase II (MII) oocytes in numbers similar to those of the control mice (Fig. S1C,D). These ovulated *Dcaf2*-null oocytes contained normal spindles (Fig. S1D). When the GV stage-arrested fully grown *Dcaf2*-null oocytes were isolated and cultured *in vitro*, they had normal germinal vesicle breakdown (GVBD) and polar body-1 (PB1) emission rates, just as the control oocytes did (Fig. S1E). These results suggested that *Dcaf2* is dispensable for oocyte survival from the primordial-follicle stage to ovulation; the loss of DCAF2 did not affect oocyte meiotic maturation.

In a rescue experiment, when the *Dcaf2^{♀-/-♂+}* zygotes were microinjected with exogenous *Dcaf2* mRNAs (mCherry-*Dcaf2*) and cultured *in vitro*, they could develop into blastocysts with significantly higher efficiency than the control zygotes (*Dcaf2^{♀-/-♂+}* zygotes microinjected with mRNAs encoding for mCherry) (Fig. 1G,H). This result further indicated that maternal DCAF2 is specifically needed in zygotes but is dispensable for oocyte development and survival.

Maternal *Dcaf2* is required for the maintenance of genome stability and for repression of DNA over-replication in zygotes

We then investigated the reason for the developmental arrest of *Dcaf2^{♀-/-♂+}* zygotes. DNA damage labeled with S139-phosphorylated histone H2AX (pH2AX-S139, also known as γ H2AX) was detected in WT zygotes at the pronucleus (PN)-4 stage (Fig. 2A) but was

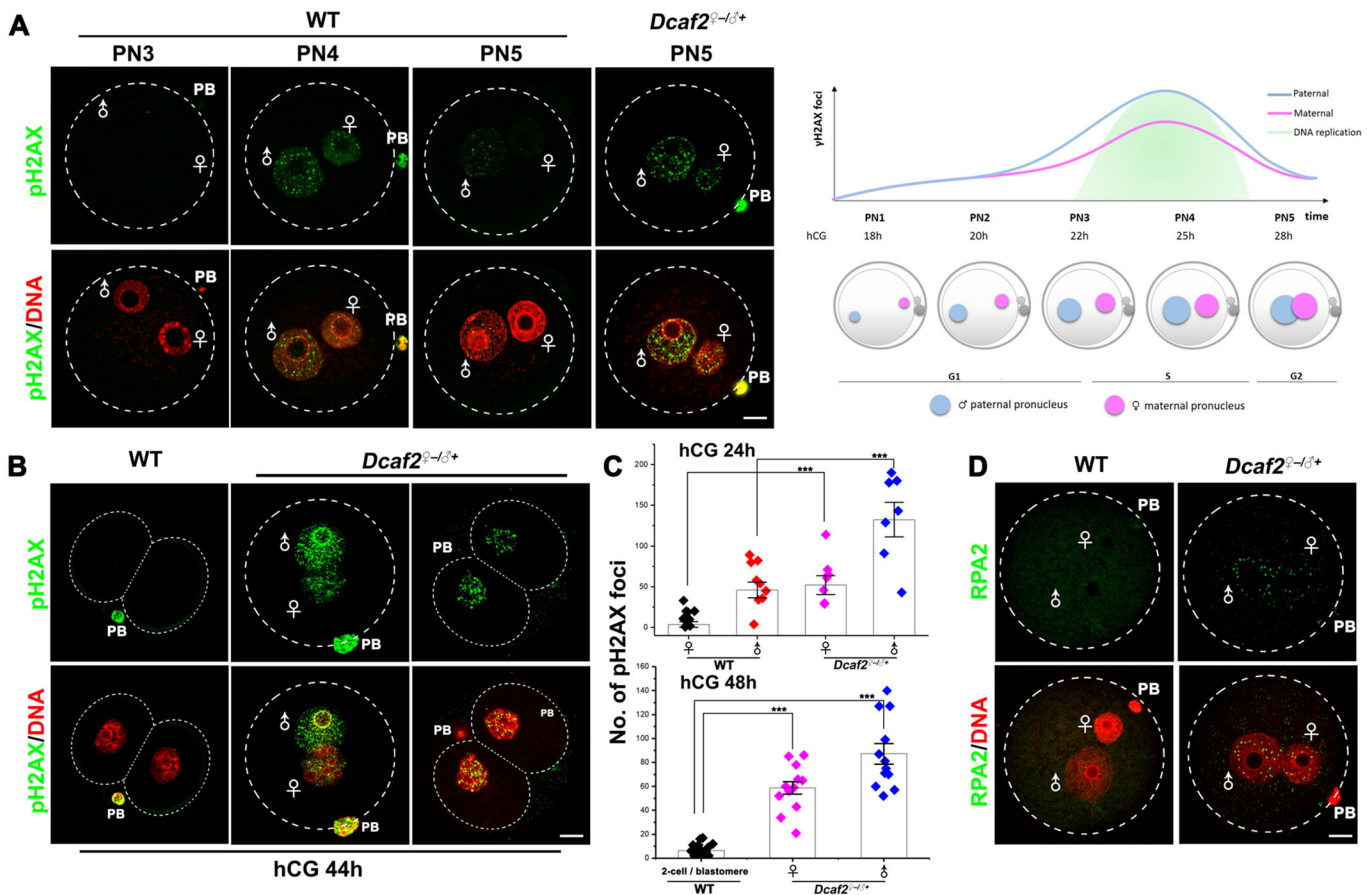


Fig. 2. Maternal *Dcaf2* deletion causes DNA damage accumulation in zygotes. (A, B) pH2AX immunofluorescence showing DNA damage in WT and *Dcaf2^{♀-/-♂+}* embryos at the indicated developmental stages. The dynamics of DNA damage and DNA replication coupled to zygotic development are illustrated in the right panel in A. ♀ and ♂ indicate maternal or paternal pronuclei, respectively. (C) Quantification of pH2AX foci in male and female pronuclei of WT and *Dcaf2^{♀-/-♂+}* embryos. For two-cell embryos, pH2AX foci in the nucleus of each blastomere were counted; pH2AX foci in ≥ 10 embryos were counted in each experimental group. Data are mean \pm s.e.m. *** $P < 0.001$ by two-tailed Student's *t*-test. (D) RPA2 immunofluorescence results showing DNA single-strand breaks in WT and *Dcaf2^{♀-/-♂+}* zygotes; ≥ 10 zygotes of each genotype were observed with similar results. Scale bars: 10 μ m.

repaired in two-cell embryos (Fig. 2B). By contrast, the *Dcaf2*^{♀-/-σ⁺} zygotes contained stronger pH2AX signals than the WT zygotes did at PN5 (Fig. 2A), and the signals increased further when the control embryos developed to two-cell stage (Fig. 2B). The pH2AX foci in male/female pronuclei were counted, and the numbers are shown in Fig. 2C. Occasionally, a few *Dcaf2*^{♀-/-σ⁺} zygotes divided once but were arrested at the two-cell stage. These embryos contained abundant pH2AX signals in nuclei, while the control two-cell embryos were negative for pH2AX (Fig. 2B). In addition, RPA2, a marker of single-strand DNA breaks, was detected in *Dcaf2*^{♀-/-σ⁺} zygotes but not in WT zygotes (Fig. 2D). When we

overexpressed exogenous DCAF2 in *Dcaf2*^{♀-/-σ⁺} zygotes, the formation of pH2AX foci was significantly repressed, indicating that the accumulation of DNA damage is a direct effect of maternal DCAF2 depletion (Fig. S2).

It has been reported that mammalian DCAF2 prevents DNA re-replication in cultured cancer cell lines (Pan et al., 2013). Therefore, we assessed the possible role of maternal DCAF2 in the regulation of the first round of DNA replication in zygotes. BrdU incorporation data indicated that DNA replication in WT zygotes was initiated at the PN3 stage and finished at the early PN5 stage (6 h and 12 h after *in vitro* fertilization, respectively; Fig. 3A).

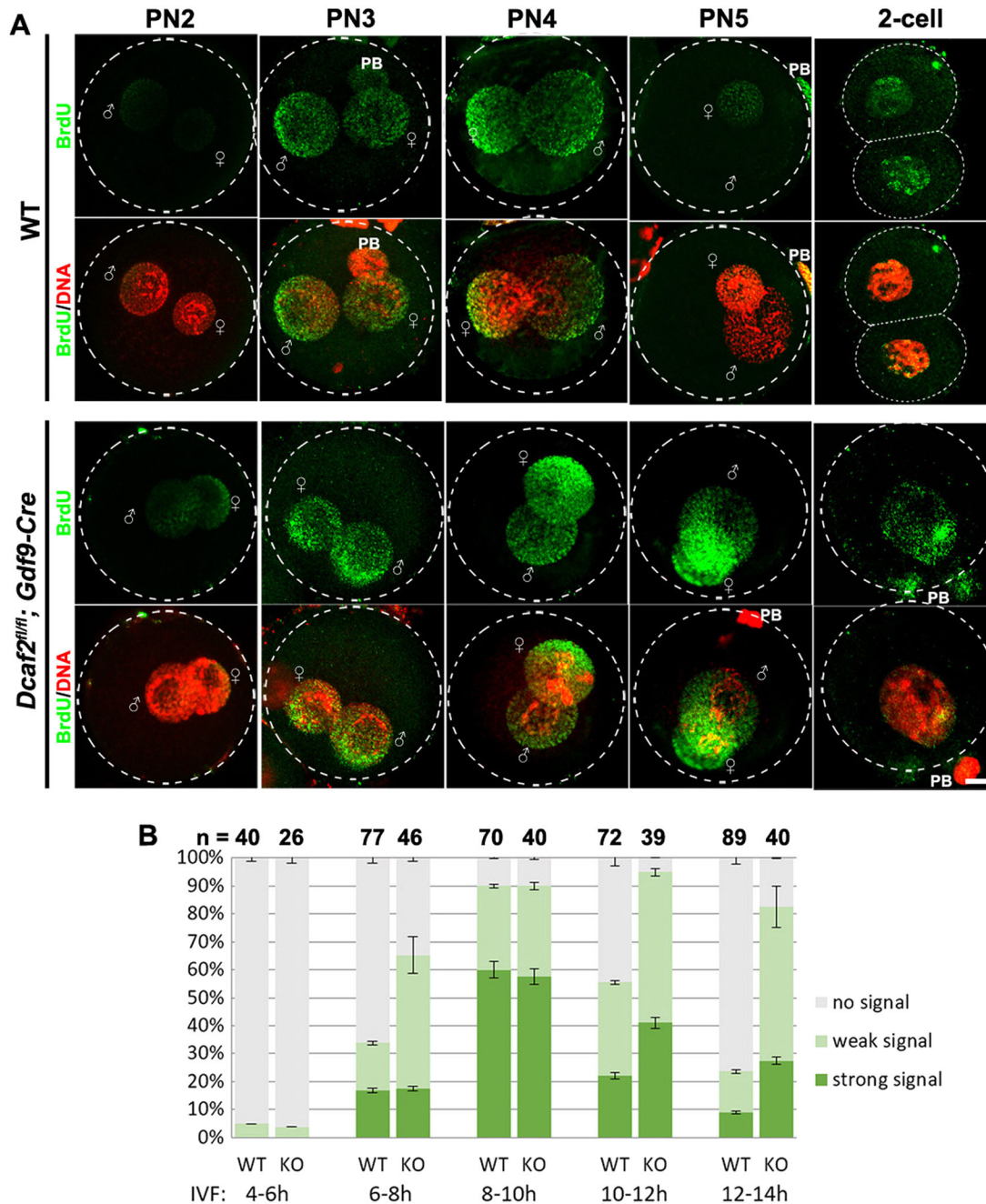


Fig. 3. Maternal *Dcaf2* deletion leads to DNA over-replication and zygotic developmental arrest. (A,B) BrdU incorporation assay showing DNA replication processes in WT and *Dcaf2*^{♀-/-σ⁺} zygotes. *In vitro* fertilized eggs at each developmental stage were incubated in medium containing BrdU for 2 h before immunofluorescent staining (A). Zygotes with weak and strong BrdU signals were quantified (B). Numbers of zygotes observed at each developmental stage are indicated. Scale bar: 10 μm.

Nevertheless, DNA replication was initiated early in *Dcaf2*^{♀-/-σ+} zygotes at PN2 stage and did not stop at the late PN5 stage. Even when the control zygotes developed to the two-cell stage and started the second round of DNA replication, BrdU incorporation was still detectable in developmentally arrested *Dcaf2*^{♀-/-σ+} zygotes (Fig. 3A,B).

The DNA replication licensing factor CDT1 has been reported to be a target of CRL4^{DCAF2} in the maintenance of genome integrity of proliferating somatic cells (Shibata et al., 2011). CDT1 is degraded by CRL4^{DCAF2} after S phase entry to ensure that DNA replicates only once per cell cycle (Kim et al., 2008). We tested whether CDT1 might be involved in maternal *Dcaf2* knockout-

induced zygotic genome instability. Unfortunately, the available commercial anti-CDT1 antibodies failed to detect endogenous CDT1 in the mouse zygotes. Therefore, we expressed GFP-CDT1 in oocytes and zygotes by mRNA microinjection, to study its localization and cellular effects. Overexpressed CDT1 was localized in GV of fully grown oocytes but did not affect meiotic maturation (Fig. S3). We also expressed GFP-CDT1 in WT and *Dcaf2*^{♀-/-σ+} zygotes by mRNA microinjection. The exogenous GFP-CDT1 was strongly expressed in zygotes of both phenotypes at 7 h after microinjection, and located in both male and female pronuclei (Fig. 4A). GFP-CDT1 proteins were unstable and were remarkably degraded in WT zygotes at 21–

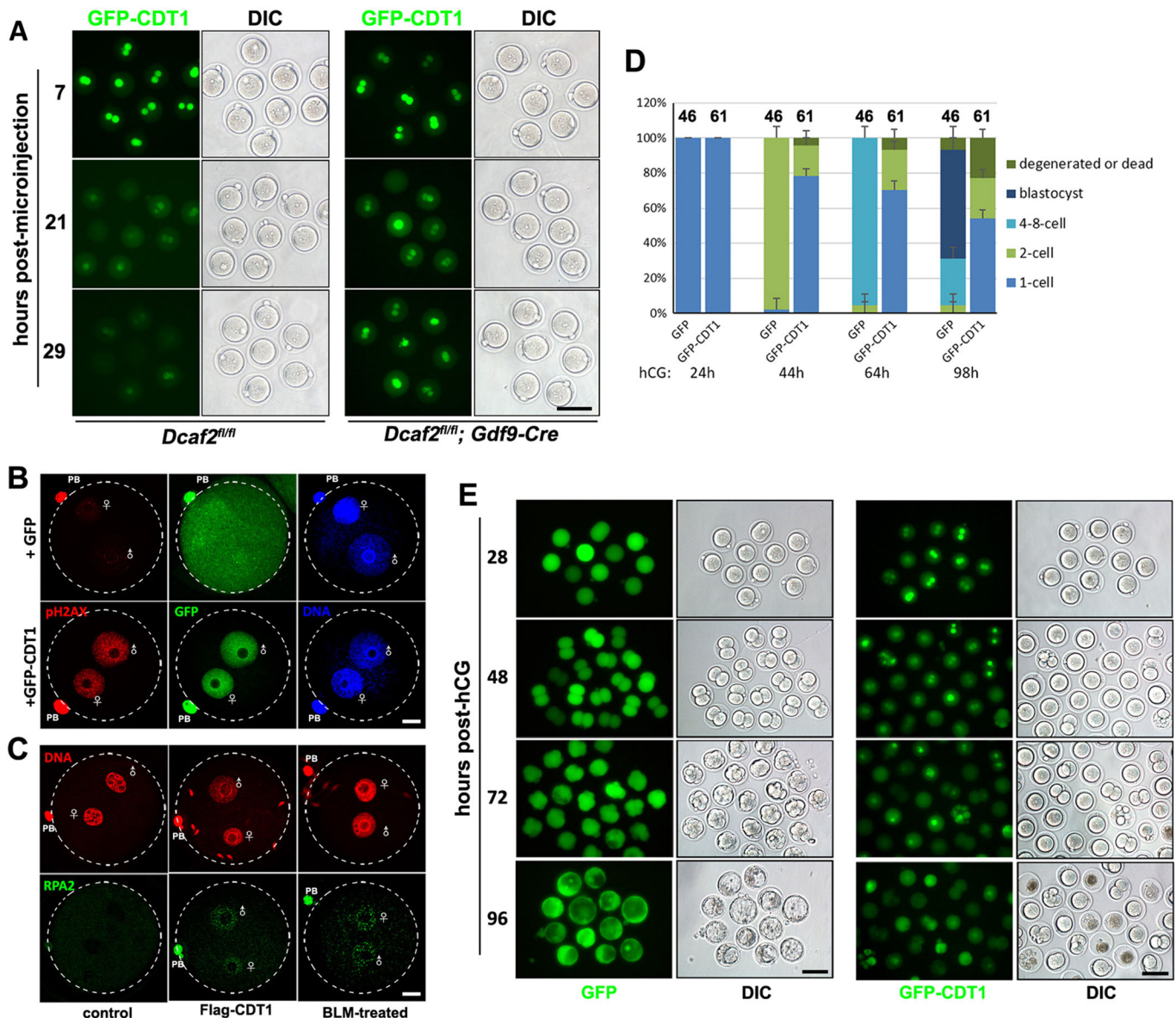


Fig. 4. Involvement of CDT1 in the zygotic developmental arrest caused by maternal *Dcaf2* deletion. (A) Stability of GFP-CDT1 in WT and *Dcaf2*^{♀-/-σ+} zygotes. WT and *Dcaf2*^{♀-/-σ+} zygotes at 14 h after hCG injection were microinjected with mRNAs encoding GFP-CDT1, and further cultured *in vitro*. The GFP signals were observed at 7, 21 and 29 h after microinjection; ≥15 zygotes of each genotype were observed with similar results. (B) Immunofluorescence results of pH2AX in zygotes microinjected with mRNAs encoding GFP (as a control) or GFP-CDT1. (C) Immunofluorescence results of RPA2 in zygotes microinjected with mRNAs encoding Flag-tagged CDT1. Bleomycin (BLM)-treated zygotes (5 mg/ml for 1 h) were stained as a positive control of DNA damage signals; ≥15 zygotes in each treatment group were observed with similar results. (D,E) Quantification of developmental rates (D) and representative images (E) showing that CDT1 overexpression caused zygotic developmental arrest. Numbers of zygotes injected with mRNAs encoding for GFP (as a control) or GFP-CDT1 are indicated. Scale bars: 10 μm in B and C; 100 μm in A and E.

29 h after microinjection. By contrast, the exogenous GFP-CDT1 remained stable in *Dcaf2*^{♀-/-♂+} zygotes at these time points (Fig. 4A). This result provided direct evidence that loss of DCAF2 led to the persistence of CDT1 in zygotes.

Significantly, overexpression of CDT1 in zygotes induced massive DNA damage, as revealed by pH2AX and RPA2 immunofluorescence assays (Fig. 4B,C), and caused developmental arrest at one- to two-cell stages (Fig. 4D,E). Thus, CDT1 overexpression in oocytes and zygotes mimicked the phenotypes of maternal *Dcaf2* deletion. This observation suggested that DCAF2 maintains zygotic genome stability by downregulating CDT1 in the first mitotic cell cycle.

The involvement of *Dcaf2* in DNA modification, histone modification and histone exchange during maternal-zygotic transition

Because DNA replication, DNA damage and DNA demethylation are interacting events in zygotes (Hajkova et al., 2010), we evaluated the potential effects of *Dcaf2* deletion on epigenetic modifications in oocytes and zygotes. The oocytes of *Dcaf2*^{fl/fl}; *Gdf9-Cre* mice had similar numbers of DNA 5-methylcytosine (5mC)-to-5-hydroxymethylcytosine (5hmC) modifications (Fig. S4A). In WT zygotes, 5hmC levels were higher in male pronuclei than in female pronuclei, while 5mC levels showed the opposite trend. Nonetheless, female pronuclear 5hmC signals were remarkably increased in *Dcaf2*^{♀-/-♂+} zygotes (Fig. 5A).

Our results suggested that formation of both DNA double-strand breaks and 5hmC in WT zygotes was more active in the male

pronucleus than in the female pronucleus, and that both signals were upregulated in the female pronucleus of *Dcaf2*^{♀-/-♂+} zygotes, suggesting that DNA damage and DNA demethylation may correlate. To confirm this notion, we examined pH2AX amounts in zygotes derived from *Ddb1*^{fl/fl}; *Gdf9-Cre* mice, in which the DNA demethylase methylcytosine dioxygenase (TET3) is inactive and 5hmC fails to accumulate in the male pronucleus (Yu et al., 2013). No pH2AX foci were detected in these zygotes at PN3–5 stages (Fig. 5B). This result indicated that drastic DNA modifications induce DNA damage in the zygotic genome, and maternally expressed DCAF2 is required for repair of this DNA damage to ensure normal development (Fig. 5C).

On the other hand, zygotic histone exchange and histone methylation were not affected by the maternal *Dcaf2* knockout. After fertilization, *de novo* synthesized histone H3.3 could load onto chromatin of both male and female pronuclei (Fig. S4B), and histone methylation markers H3K4me3 and H3K9me3 showed a normal distribution pattern (more abundant in the female than male pronucleus) in *Dcaf2*-deleted zygotes (Fig. S4C).

Inhibition of DNA replication enhanced DNA damage in both WT and *Dcaf2*^{♀-/-♂+} zygotes

The data above showed that both DNA over-replication and genome reprogramming contributed to the accumulation of DNA damage in *Dcaf2*^{♀-/-♂+} zygotes. To determine whether suppression of DNA replication can protect *Dcaf2*^{♀-/-♂+} zygotes from DNA damage, we treated zygotes with aphidicolin (5 μM), a specific inhibitor of DNA polymerase α. Aphidicolin efficiently blocked DNA replication

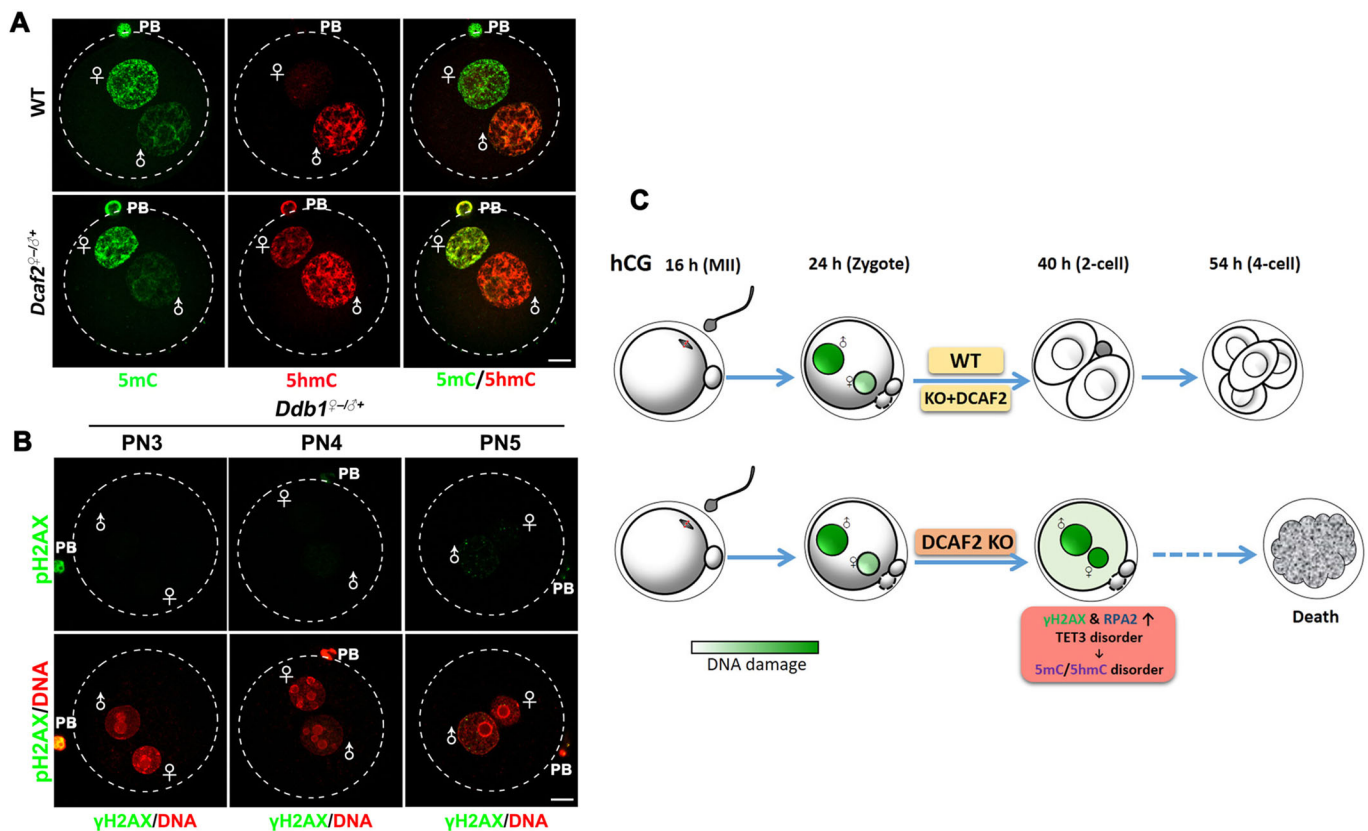


Fig. 5. Levels of DNA methylation/demethylation and DNA damage in WT and *Dcaf2*^{♀-/-♂+} zygotes. (A) 5mC and 5hmC immunofluorescence results showing DNA 5mC and 5hmC distributions in male and female pronuclei of WT and *Dcaf2*^{♀-/-♂+} zygotes. (B) pH2AX immunofluorescence results showing loss of DNA damage in *Ddb1*^{fl/fl}; *Gdf9-Cre* zygotes at the indicated developmental stages. (C) Schematic of DCAF2 involvement in the repair of DNA damage during embryo development. Scale bars: 10 μm.

because bromodeoxyuridine (BrdU) incorporation was abrogated in the aphidicolin-treated zygotes (Fig. 6A). Nonetheless, aphidicolin treatment did not reduce DNA damage signals in *Dcaf2*^{♀-/-♂+}

zygotes. Instead, DNA damage labeled with pH2AX increased in both WT and *Dcaf2*^{♀-/-♂+} zygotes after aphidicolin treatment (Fig. 6B). In addition, immunofluorescence data revealed that

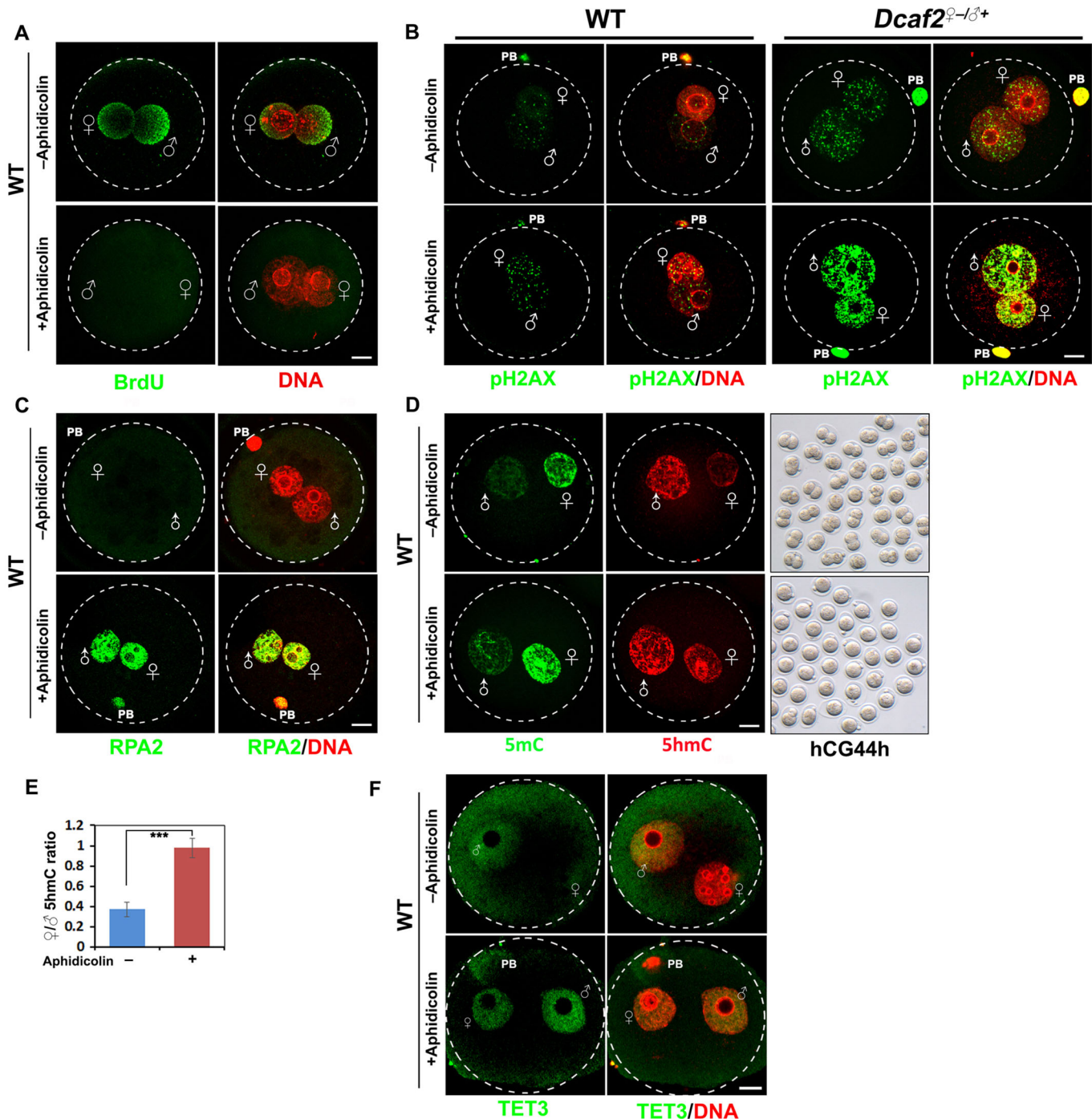


Fig. 6. Inhibition of DNA replication failed to rescue DNA damage in maternal *Dcaf2*-deleted zygotes. (A) Aphidicolin treatment blocked DNA replication in WT zygotes so that BrdU incorporation into genome DNA was not detected. Fertilized eggs from superovulated females at 16 h after hCG injection (mostly at PN3 stage) were cultured in KSOM with or without 5 μ M aphidicolin. (B) Immunofluorescent staining for pH2AX in WT and *Dcaf2*^{♀-/-♂+} zygotes with or without aphidicolin treatment. Zygotes were collected and treated as in A. (C) RPA2 immunofluorescence in WT zygotes with or without aphidicolin treatment. (D) 5mC and 5hmC immunofluorescence in WT zygotes with or without aphidicolin treatment. Differential interference contrast (DIC) images (right column) showed that the untreated zygotes developed into two-cell embryos 44 h after hCG injection, while the aphidicolin-treated zygotes were arrested at the one-cell stage. (E) Quantification of 5hmC/5mC ratio between female and male pronuclei. The brightness of 5hmC per field in the female pronucleus divided by that in the male pronucleus was calculated by ImageJ. *n*=10 for each experimental group. Data are mean \pm s.e.m. ****P*<0.001 by two-tailed Student's *t*-test. (F) TET3 immunofluorescence in zygotes with or without aphidicolin treatment. For each experimental group, \geq 10 zygotes were observed with similar results. Scale bars: 10 μ m.

RPA2, a marker of DNA single-strand breaks, was undetectable in normal WT zygotes but was significantly upregulated in aphidicolin-treated zygotes (Fig. 6C). Therefore, inhibiting DNA polymerase activity caused DNA replication stress and massive DNA damage instead of preventing it. In comparison with WT zygotes, *Dcaf2*^{2-/-} zygotes are more susceptible to aphidicolin-induced DNA damage (Fig. 6B); this finding implied that they are more fragile and have an insufficient DNA repair ability in response to environmental stressors.

Moreover, the DNA 5hmC amount also increased in zygotes incubated with aphidicolin (Fig. 5D). Under DNA replication stress, the asymmetrical 5hmC distribution between male and female pronuclei disappeared, and the embryos were arrested at the one-cell stage (Fig. 6D). This phenotype is similar to the one we observed in *Dcaf2*^{2-/-} zygotes. The ratio of female to male pronuclear 5hmC intensities was ~0.4 in control zygotes but increased to ~1.0 in aphidicolin-treated zygotes (Fig. 6E). The DNA demethylase TET3 that mediates 5hmC formation in zygotes was preferentially localized to male pronuclei of control zygotes (Gu et al., 2011), but was evenly distributed in male and female pronuclei of aphidicolin-treated zygotes, as shown by immunofluorescence using a TET3 antibody kindly provided by Dr Guoliang Xu (State Key Laboratory of Molecular Biology, Shanghai, China) (Fig. 6F). Therefore, DCAF2 deletion-induced or DNA polymerase inhibition-induced DNA replication stress impaired the asymmetrical TET3 localization in pronuclei and led to increased 5hmC generation in the female pronucleus.

Dcaf2-null oocytes are susceptible to DNA-damaging insults

Although *Dcaf2* is not required for oocyte survival and meiotic maturation in a normal physiological environment, *Dcaf2*-null oocytes might be vulnerable to DNA-damaging stressors. To test this hypothesis, we used the anticancer drug etoposide, also known as VP-16, to induce DNA double-strand breaks in WT and *Dcaf2*-null GV oocytes. The oocytes were treated with 5 μ M VP-16 for 3 h and then cultured in a VP-16-free medium (containing 2 μ M milrinone to inhibit spontaneous GVBD) for self-repair overnight (Fig. 7A). VP-16 induced massive DNA damage, which was repaired fully in WT oocytes but not in *Dcaf2*-null oocytes after overnight culture (Fig. 7B,C). These results indicated that DCAF2 was recruited to repair DNA damage in GV oocytes, but its specific biochemical function in this process has yet to be determined.

DISCUSSION

The gene encoding DCAF2 was first discovered in yeast in 2003, and was later shown to be evolutionarily conserved and to perform key functions in the maintenance of genome stability (Jascur et al., 2011; Kim et al., 2008; Yoshida et al., 2003). On the other hand, its participation in postnatal development and hemostasis has never been studied *in vivo*, owing to the early mortality of *Dcaf2* knockout embryos at the ~eight-cell stage (Liu et al., 2007). After generating a novel *Dcaf2*-floxed mouse strain, we studied the function of *Dcaf2* in germ cells for the first time.

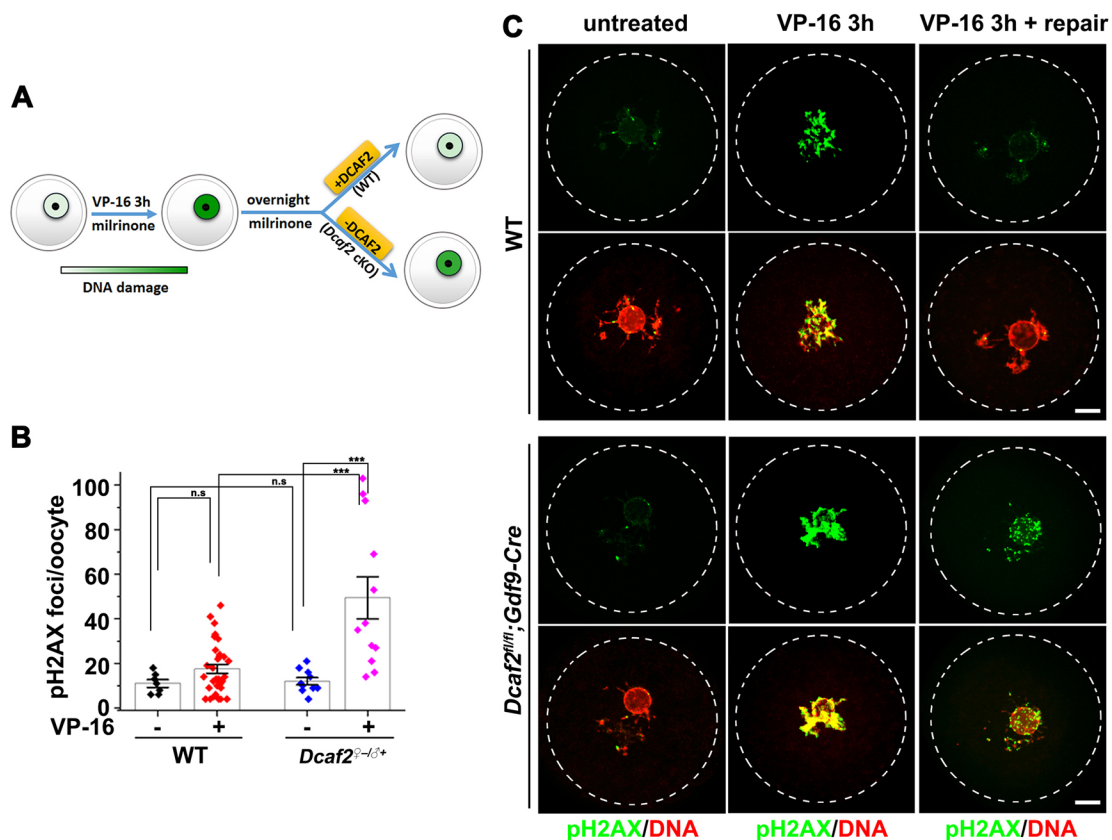


Fig. 7. *Dcaf2*-deleted oocytes are vulnerable to DNA damage insults. (A) Schematic of the experimental design and conclusions for B and C. (B,C) Oocytes were treated with 5 mg/ml VP-16 for 3 h to induce DNA damage and then released from VP-16 for self-repair overnight. pH2AX immunofluorescence (C) showing that DNA damage was repaired to normal levels in WT oocytes but not in *Dcaf2*-deleted oocytes. The numbers of pH2AX foci per oocyte after each treatment are quantified in B; ≥ 10 oocytes were observed in each experimental group. Data are mean \pm s.e.m. *** $P < 0.001$ by two-tailed Student's *t*-test. n.s., nonsignificant. Scale bars: 10 μ m.

Although DCAF2 appears to be necessary for survival and proliferation of cultured somatic cells, it is dispensable for oocyte growth and meiotic maturation (Coleman et al., 2015). This phenomenon is likely to be caused by the dormancy of DNA replication in oocytes. DCAF2 is mainly a nuclear protein in somatic cells but was found to be evenly distributed in GV oocytes, further suggesting that it is functionally inactive at this developmental stage (Pan et al., 2013). This novel finding suggests that DCAF2 is required only for maintenance of genome integrity during the S phase of the cell cycle. Currently, we do not know whether oocytes are the only nonproliferating cell type tolerant of *Dcaf2* deletion. It will be interesting to determine whether DCAF2 is also dispensable in other terminally differentiated cell types arrested in the G0 phase, such as neurons, hepatocytes and adipocytes, by means of a tissue-specific knockout using the *Dcaf2*-floxed mice reported in this study.

Our study also identified DCAF2 as a previously unrecognized maternal factor that safeguards zygotic genome stability. Accompanying the initiation of the first round of zygotic DNA replication, maternal DCAF2 molecules translocate from the cytoplasm into pronuclei, indicating their functional activation in the S phase. Maternal *Dcaf2*-deleted embryos were arrested at one- to two-cell stages owing to prolonged DNA replication and accumulation of massive DNA damage. Biochemically, DCAF2 could play two roles in the maintenance of zygotic genome integrity. First, drastic genome reprogramming in zygotes, particularly in the male pronucleus, causes DNA double-strand breaks; DCAF2 may be directly involved in the timely repair of these DNA lesions to ensure embryonic cell cycle progression, as has been observed in cultured somatic cells (Blaikley et al., 2014; Han et al., 2015). Second, DCAF2 functions as a substrate adaptor mediating CRL4-dependent ubiquitylation and degradation of the DNA replication licensing factor CDT1, thereby preventing the DNA damage caused by re-replication (Higa et al., 2006; Jin et al., 2006). CDT1 overexpression in WT zygotes mimicked the phenotype of *Dcaf2*^{♀-σ+} zygotes, indicating that maintaining appropriate CDT1 amounts is indeed crucial for zygotic cell cycle progression.

As we already pointed out in the Results section, most commercially available antibodies against DCAF2 and CDT1 were generated and selected to target human antigens, and therefore all failed to detect the corresponding antigens in mouse oocytes and zygotes. Owing to this technical obstacle, we could not describe fluctuations in the amount and localization changes of endogenous DCAF2 and CDT1 before and after fertilization. As a partial compensation, our results using exogenously expressed DCAF2 and CDT1 demonstrated that both proteins are stringently regulated during maternal-zygotic transition and are necessary for completion of the first mitotic cell cycle.

In addition to DNA replication and damage repair, we also studied the effects of maternal *Dcaf2* deletion on DNA and histone methylation during maternal-zygotic transition. The results indicated that although histone loading and methylation were not obviously affected in *Dcaf2*^{♀-σ+} zygotes, the asymmetrical pattern of DNA demethylation in pronuclei was disturbed (Nakamura et al., 2012). It has been demonstrated that DNA demethylase TET3 preferentially enters the male pronucleus and drives prompt DNA demethylation in the zygote (Gu et al., 2011; Yu et al., 2013). H3K9me2 on the maternal genome was reported to inhibit access of TET3 to the female PN (Nakamura et al., 2012). It would be interesting to see whether TET3 can be located in the female PN while asymmetric H3K9me2 distribution is maintained in maternal

Dcaf2 knockout zygotes. In addition, DNA repair pathways may be involved in the zygotic DNA demethylation process. There is no direct evidence that maternal DCAF2 directly regulates DNA demethylation. Rather, our results indicate that replication stress or large-scale DNA damage (caused by *Dcaf2* deletion or DNA polymerase inhibition) prevents the establishment of the asymmetrical DNA demethylation pattern in the zygote.

MATERIALS AND METHODS

Mice

Dcaf2^{fl/fl} mice were generated by the Model Animal Resource Information Platform, Model Animal Research Center of Nanjing University. Embryonic stem cells used to generate this mouse strain were purchased from the European Conditional Mouse Mutagenesis Program (ES cell clone EPD0842_C05). *Dcaf2*^{fl/fl}; *Gdf9-Cre* mice were produced by crossing mice bearing the *Dcaf2*^{fl} allele with previously reported *Gdf9-Cre* transgenic mice (Yu et al., 2013, 2016b). Mice were genotyped by PCR using genomic tail DNA. All primers used for genotyping and other applications are listed in Table S1. Animal care and experimental procedures were in accordance with the Animal Research Committee guidelines of Zhejiang University.

In vitro transcription and preparation of mRNAs for microinjections

Human *Dcaf2* cDNA from an Invitrogen cDNA library was subcloned into mCherry-tagged expression plasmids. Mouse *Cdt1* cDNA PCR-amplified from the mouse cDNA library was subcloned into GFP-tagged expression plasmids. Linearized plasmids were *in vitro* transcribed using a T7 and SP6 mMESSEAGEmMACHINE Kit (Invitrogen, AM1344 and AM1340, respectively) following the manufacturer's instructions. mRNAs were recovered by lithium chloride precipitation and resuspended in nuclease-free water.

Microinjection

For microinjection, GV oocytes were harvested in M2 medium with 2 μM milrinone to inhibit spontaneous GVBD, and zygotes were cultured in KSOM containing 20 mM HEPES. All injections were performed using an Eppendorf transferman NK2 micromanipulator. Each oocyte or zygote was injected with 5–10 pl RNA samples. After injection, oocytes or zygotes were washed and cultured at 37°C with 5% CO₂.

Superovulation and fertilization

Female mice (21–23 days old) were intraperitoneally injected with 5 IU pregnant mare serum gonadotropin (PMSG) and with 5 IU human chorionic gonadotropin (hCG) 44 h later. After an additional 16 h, oocyte/cumulus masses were surgically removed from the oviducts, and the numbers of oocytes were counted after digestion with 0.3% hyaluronidase (Sigma-Aldrich). Oocyte images were acquired using a Nikon SMZ1500 stereoscope. To obtain early embryos, superovulated females were mated with 10- to 12-week-old WT males. Successful mating was confirmed by the presence of vaginal plugs. Embryos were harvested from oviducts at the indicated times post-hCG injection. In some experiments, *in vitro* fertilization was performed as previously described to synchronize zygotic development.

Oocyte and embryo culture

Oocytes at the GV stage were harvested in M2 medium (M7167; Sigma-Aldrich) and cultured in mini-drops of M16 medium (M7292; Sigma-Aldrich) covered with mineral oil (M5310; Sigma-Aldrich) at 37°C in a 5% CO₂ atmosphere. Zygotes were harvested from fertilized females after the hCG injection, and cultured in KSOM medium (Millipore).

Immunofluorescent staining

Oocytes were fixed in 4% paraformaldehyde in PBS for 30 min at room temperature and permeabilized for 15 min in 0.3% Triton X-100 in PBS. Antibody staining was performed using standard protocols described previously (Zhang et al., 2015). The antibodies used are listed in Table S2. Imaging of embryos following immunofluorescence was performed on a Zeiss LSM710 confocal microscope.

Histological analysis

Ovaries were collected and fixed in formalin overnight, processed, and embedded in paraffin using standard protocols (Zhang et al., 2016). Ovaries were serially sectioned at 5 μ m and stained with Hematoxylin and Eosin (H&E). Immunohistochemistry was performed using standard protocols (Sha et al., 2017). The antibodies used are listed in Table S2.

BrdU incorporation assay

To detect DNA replication, zygotes were labeled at the indicated time points after fertilization with 1 mmol/l BrdU in KSOM for 2 h. The embryos were fixed in 2.5% paraformaldehyde in PBS containing 0.5 N NaOH for 15 min at room temperature. BrdU incorporation into DNA was detected with a mouse monoclonal antibody against BrdU (Table S2), followed by Alexa Fluor 488-conjugated goat anti-mouse IgG. The embryos were mounted in 80% glycerol and observed with a laser-scanning confocal microscope. Zygotes showing small foci of BrdU signals in pronuclei were defined as 'zygotes with weak BrdU signals', and those showing even BrdU signals in the whole pronuclei (excluding the nucleolus-like body) were defined as 'zygotes with strong BrdU signals'.

Western blotting

First, 100 oocytes or embryos were lysed in protein loading buffer and heated at 95°C for 5 min. Then, SDS-PAGE and immunoblotting were performed using a Mini-PROTEAN Tetra Cell System (Bio-Rad) following standard procedures (Yu et al., 2016a). The antibodies used are listed in Table S2.

Real-time RT-PCR

Total RNA was extracted from oocytes or embryos using a RNeasy Mini kit (Qiagen) according to the manufacturer's instructions, followed by reverse transcription (RT) using a Superscript RT kit (Bio-Rad). Quantitative RT-PCR was performed using a Power SYBR Green PCR Master Mix (Applied Biosystems, Life Technologies) with an ABI 7500 Real-Time PCR system (Applied Biosystems) and the primers listed in Table S1. The relative transcript level of *Dcaf2* in the control sample (left-hand bar of each graph) was set as 1 in Fig. 1A,B,E. The relative transcript levels of other samples were compared to the control, and the fold changes shown. For each experiment, quantitative PCR reactions were performed in triplicate.

Competing interests

The authors declare no competing or financial interests.

Author contributions

Conceptualization: H.-Y.F.; Methodology: X.W.; Investigation: Y.-W.X., L.-R.C., M.W.; Resources: Y.X.; Data curation: H.-Y.F.; Writing - original draft: Y.-W.X.; Writing - review & editing: C.T., H.-Y.F.; Supervision: J.L., H.-Y.F.; Funding acquisition: J.L., C.T., H.-Y.F.

Funding

This work was supported by the National Key Research and Development Program of China (2016YFC1000600, 2017YFSF1001500 and 2017YFC1001100) and National Natural Science Foundation of China (31528016, 31371449 and 31671558).

Supplementary information

Supplementary information available online at <http://jcs.biologists.org/lookup/doi/10.1242/jcs.206664.supplemental>

References

Abbas, T. and Dutta, A. (2011). CRL4Cdt2: master coordinator of cell cycle progression and genome stability. *Cell Cycle* **10**, 241-249.

Akiyama, T., Suzuki, O., Matsuda, J. and Aoki, F. (2011). Dynamic replacement of histone H3 variants reprograms epigenetic marks in early mouse embryos. *PLoS Genet.* **7**, e1002279.

Bennett, E. J., Rush, J., Gygi, S. P. and Harper, J. W. (2010). Dynamics of cullin-RING ubiquitin ligase network revealed by systematic quantitative proteomics. *Cell* **143**, 951-965.

Blaikley, E. J., Tinline-Purvis, H., Kasperek, T. R., Marguerat, S., Sarkar, S., Hulme, L., Hussey, S., Wee, B.-Y., Deegan, R. S., Walker, C. A. et al. (2014). The DNA damage checkpoint pathway promotes extensive resection and nucleotide synthesis to facilitate homologous recombination repair and genome stability in fission yeast. *Nucleic Acids Res.* **42**, 5644-5656.

Coleman, K. E., Grant, G. D., Haggerty, R. A., Brantley, K., Shibata, E., Workman, B. D., Dutta, A., Varma, D., Purvis, J. E. and Cook, J. G. (2015). Sequential replication-coupled destruction at G1/S ensures genome stability. *Genes Dev.* **29**, 1734-1746.

Gu, T.-P., Guo, F., Yang, H., Wu, H.-P., Xu, G.-F., Liu, W., Xie, Z.-G., Shi, L., He, X., Jin, S.-G. et al. (2011). The role of Tet3 DNA dioxygenase in epigenetic reprogramming by oocytes. *Nature* **477**, 606-610.

Hajkova, P., Jeffries, S. J., Lee, C., Miller, N., Jackson, S. P. and Surani, M. A. (2010). Genome-wide reprogramming in the mouse germ line entails the base excision repair pathway. *Science* **329**, 78-82.

Han, C., Wani, G., Zhao, R., Qian, J., Sharma, N., He, J., Zhu, Q., Wang, Q.-E. and Wani, A. A. (2015). Cdt2-mediated XPG degradation promotes gap-filling DNA synthesis in nucleotide excision repair. *Cell Cycle* **14**, 1103-1115.

Havens, C. G. and Walter, J. C. (2011). Mechanism of CRL4(Cdt2), a PCNA-dependent E3 ubiquitin ligase. *Genes Dev.* **25**, 1568-1582.

Higa, L. A., Banks, D., Wu, M., Kobayashi, R., Sun, H. and Zhang, H. (2006). L2DTL/CDT2 interacts with the CUL4/DBB1 complex and PCNA and regulates CDT1 proteolysis in response to DNA damage. *Cell Cycle* **5**, 1675-1680.

Jascur, T., Fotedar, R., Greene, S., Hotchkiss, E. and Boland, C. R. (2011). N-methyl-N'-nitro-N-nitrosoguanidine (MNNG) triggers MSH2 and Cdt2 protein-dependent degradation of the cell cycle and mismatch repair (MMR) inhibitor protein p21Waf1/Cip1. *J. Biol. Chem.* **286**, 29531-29539.

Jin, J., Arias, E. E., Chen, J., Harper, J. W. and Walter, J. C. (2006). A family of diverse Cul4-Ddb1-interacting proteins includes Cdt2, which is required for S phase destruction of the replication factor Cdt1. *Mol. Cell* **23**, 709-721.

Kim, Y., Starostina, N. G. and Kipreos, E. T. (2008). The CRL4Cdt2 ubiquitin ligase targets the degradation of p21Cip1 to control replication licensing. *Genes Dev.* **22**, 2507-2519.

Kopanja, D., Roy, N., Stoyanova, T., Hess, R. A., Bagchi, S. and Raychaudhuri, P. (2011). Cul4A is essential for spermatogenesis and male fertility. *Dev. Biol.* **352**, 278-287.

Lee, J. and Zhou, P. (2007). DCAFs, the missing link of the CUL4-DDB1 ubiquitin ligase. *Mol. Cell* **26**, 775-780.

Liu, C.-L., Yu, I.-S., Pan, H.-W., Lin, S.-W. and Hsu, H.-C. (2007). L2dtl is essential for cell survival and nuclear division in early mouse embryonic development. *J. Biol. Chem.* **282**, 1109-1118.

Ma, X.-S., Lin, F., Wang, Z.-W., Hu, M.-W., Huang, L., Meng, T.-G., Jiang, Z.-Z., Schatten, H., Wang, Z.-B. and Sun, Q.-Y. (2016). Geminin deletion in mouse oocytes results in impaired embryo development and reduced fertility. *Mol. Biol. Cell* **27**, 768-775.

Missiaglia, E., Selfe, J., Hamdi, M., Williamson, D., Schaaf, G., Fang, C., Koster, J., Summersgill, B., Messahel, B., Versteeg, R. et al. (2009). Genomic imbalances in rhabdomyosarcoma cell lines affect expression of genes frequently altered in primary tumors: an approach to identify candidate genes involved in tumor development. *Genes Chromosomes Cancer* **48**, 455-467.

Murai, S., Katagiri, Y. and Yamashita, S. (2014). Maturation-associated Dbf4 expression is essential for mouse zygotic DNA replication. *Dev. Growth Differ.* **56**, 625-639.

Nakamura, T., Liu, Y. J., Nakashima, H., Umehara, H., Inoue, K., Matoba, S., Tachibana, M., Ogura, A., Shinkai, Y. and Nakano, T. (2012). PGC7 binds histone H3K9me2 to protect against conversion of 5mC to 5hmC in early embryos. *Nature* **486**, 415-419.

Nakatani, T., Yamagata, K., Kimura, T., Oda, M., Nakashima, H., Hori, M., Sekita, Y., Arakawa, T., Nakamura, T. and Nakano, T. (2015). Stella preserves maternal chromosome integrity by inhibiting 5hmC-induced gammaH2AX accumulation. *EMBO Rep.* **16**, 582-589.

Pan, W.-W., Zhou, J.-J., Yu, C., Xu, Y., Guo, L.-J., Zhang, H.-Y., Zhou, D., Song, F.-Z. and Fan, H.-Y. (2013). Ubiquitin E3 ligase CRL4(CDT2/DCAF2) as a potential chemotherapeutic target for ovarian surface epithelial cancer. *J. Biol. Chem.* **288**, 29680-29691.

Sha, Q.-Q., Dai, X.-X., Dang, Y., Tang, F., Liu, J., Zhang, Y.-L. and Fan, H.-Y. (2017). A MAPK cascade couples maternal mRNA translation and degradation to meiotic cell cycle progression in mouse oocytes. *Development* **144**, 452-463.

Shibata, E., Abbas, T., Huang, X., Wohlschlegel, J. A. and Dutta, A. (2011). Selective ubiquitylation of p21 and Cdt1 by UBCH8 and UBE2G ubiquitin-conjugating enzymes via the CRL4Cdt2 ubiquitin ligase complex. *Mol. Cell. Biol.* **31**, 3136-3145.

Smallwood, S. A. and Kelsey, G. (2012). De novo DNA methylation: a germ cell perspective. *Trends Genet.* **28**, 33-42.

Swiech, L., Kisiel, K., Czolowska, R., Zientarski, M. and Borsuk, E. (2007). Accumulation and dynamics of proteins of the MCM family during mouse oogenesis and the first embryonic cell cycle. *Int. J. Dev. Biol.* **51**, 283-295.

Ueki, T., Nishidate, T., Park, J. H., Lin, M. L., Shimo, A., Hirata, K., Nakamura, Y. and Katagiri, T. (2008). Involvement of elevated expression of multiple cell-cycle regulator, DTL/RAMP (denticleless/RA-regulated nuclear matrix associated protein), in the growth of breast cancer cells. *Oncogene* **27**, 5672-5683.

Wang, Z.-W., Ma, X.-S., Ma, J.-Y., Luo, Y.-B., Lin, F., Wang, Z.-B., Fan, H.-Y., Schatten, H. and Sun, Q.-Y. (2013). Laser microbeam-induced DNA damage inhibits cell division in fertilized eggs and early embryos. *Cell Cycle* **12**, 3336-3344.

- Xu, Q., Wang, F., Xiang, Y., Zhang, X., Zhao, Z.-A., Gao, Z., Liu, W., Lu, X., Liu, Y., Yu, X.-J. et al. (2015). Maternal BCAS2 protects genomic integrity in mouse early embryonic development. *Development* **142**, 3943-3953.
- Yoshida, S. H., Al-Amodi, H., Nakamura, T., McInerney, C. J. and Shimoda, C. (2003). The Schizosaccharomyces pombe cdt2(+) gene, a target of G1-S phase-specific transcription factor complex DSC1, is required for mitotic and premeiotic DNA replication. *Genetics* **164**, 881-893.
- Yu, C., Zhang, Y.-L., Pan, W.-W., Li, X.-M., Wang, Z.-W., Ge, Z.-J., Zhou, J.-J., Cang, Y., Tong, C., Sun, Q.-Y. et al. (2013). CRL4 complex regulates mammalian oocyte survival and reprogramming by activation of TET proteins. *Science* **342**, 1518-1521.
- Yu, C., Ji, S.-Y., Sha, Q.-Q., Sun, Q.-Y. and Fan, H.-Y. (2015a). CRL4-DCAF1 ubiquitin E3 ligase directs protein phosphatase 2A degradation to control oocyte meiotic maturation. *Nat. Commun.* **6**, 8017.
- Yu, C., Xu, Y.-W., Sha, Q.-Q. and Fan, H.-Y. (2015b). CRL4DCAF1 is required in activated oocytes for follicle maintenance and ovulation. *Mol. Hum. Reprod.* **21**, 195-205.
- Yu, C., Ji, S.-Y., Sha, Q.-Q., Dang, Y., Zhou, J.-J., Zhang, Y.-L., Liu, Y., Wang, Z.-W., Hu, B., Sun, Q.-Y. et al. (2016a). BTG4 is a meiotic cell cycle-coupled maternal-zygotic-transition licensing factor in oocytes. *Nat. Struct. Mol. Biol.* **23**, 387-394.
- Yu, J., Lan, X., Chen, X., Yu, C., Xu, Y., Liu, Y., Xu, L., Fan, H.-Y. and Tong, C. (2016b). Protein synthesis and degradation are essential to regulate germline stem cell homeostasis in Drosophila testes. *Development* **143**, 2930-2945.
- Zhang, H. and Liu, K. (2015). Cellular and molecular regulation of the activation of mammalian primordial follicles: somatic cells initiate follicle activation in adulthood. *Hum. Reprod. Update* **21**, 779-786.
- Zhang, Y.-L., Liu, X.-M., Ji, S.-Y., Sha, Q.-Q., Zhang, J. and Fan, H.-Y. (2015). ERK1/2 activities are dispensable for oocyte growth but are required for meiotic maturation and pronuclear formation in mouse. *J. Genet. Genomics* **42**, 477-485.
- Zhang, Y.-L., Guo, K.-P., Ji, S.-Y., Liu, X.-M., Wang, P., Wu, J., Gao, L., Jiang, T.-Q., Xu, T. and Fan, H.-Y. (2016). Development and characterization of a novel long-acting recombinant follicle stimulating hormone agonist by fusing Fc to an FSH-beta subunit. *Hum. Reprod.* **31**, 169-182.

Supplemental information

Supplemental figures

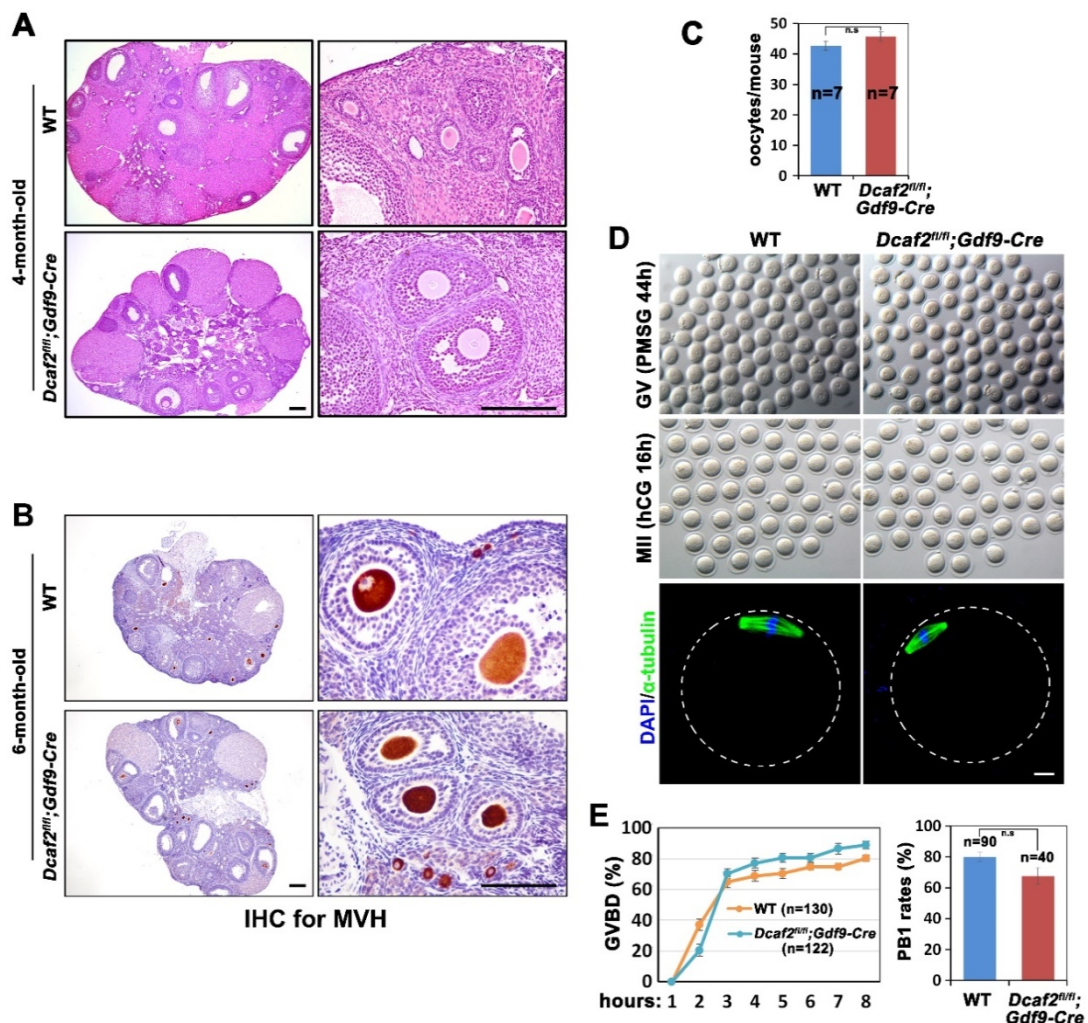


Figure S1: Generation and characterization of *Dcaf2^{fl/fl};Gdf9-Cre* mice.

A-B: H&E staining (**A**) and MVH immunohistochemistry (**B**) showing that oocyte survival and follicle development are not affected in the ovaries of adult *Dcaf2^{fl/fl};Gdf9-Cre* mice. Scale bar = 200 μ m. **C:** Numbers of oocytes collected from oviducts of WT and *Dcaf2^{fl/fl};Gdf9-Cre* mice (23-day-old) at 16 h after superovulation. N = 7 for each genotype. **D:** Fully grown GV oocytes and mature MII oocytes collected from antral follicles (GV) and oviducts (MII) of WT and *Dcaf2^{fl/fl};Gdf9-Cre* mice. The spindles in MII oocytes were labeled by immunofluorescent staining of α -tubulin, and DNA was stained by DAPI. Scale bar = 10 μ m. **E:** GVBD and PB1 emission rates of in vitro cultured oocytes from WT and *Dcaf2^{fl/fl};Gdf9-Cre* mice.

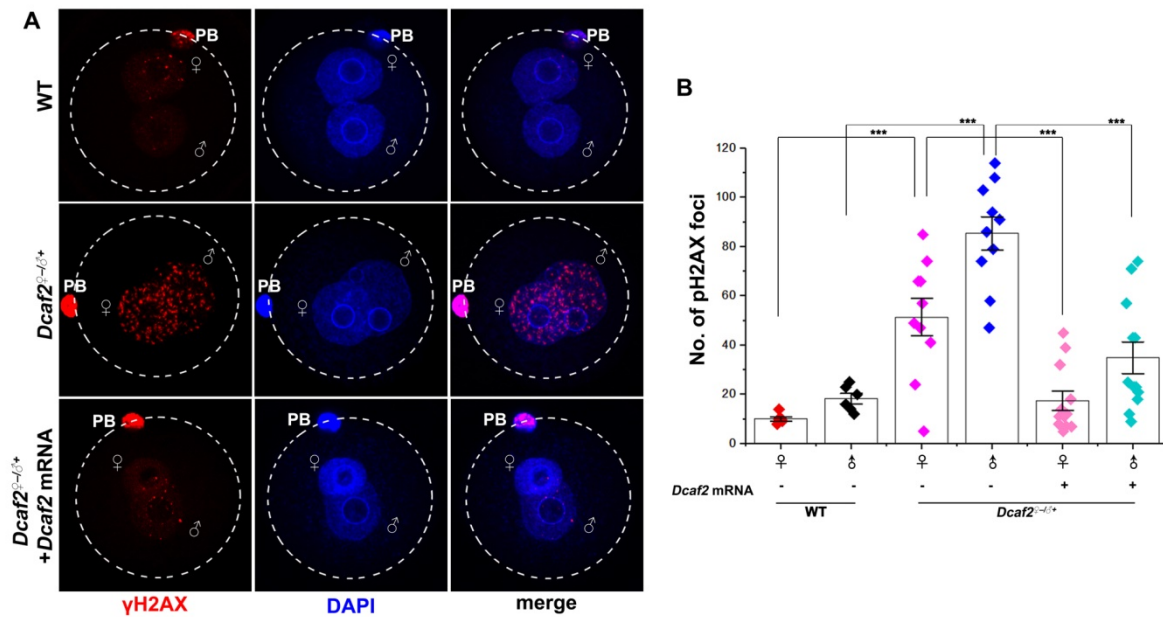


Figure S2: DCAF2 overexpression in $Dcaf2^{\text{♀}/\text{♂}^+}$ zygotes repressed the formation of pH2AX foci.

A: Localization of pH2AX in zygotes at PN5 stage. $Dcaf2^{\text{♀}/\text{♂}^+}$ zygotes were collected from oviducts at 14 h after hCG injection, and microinjected with mRNAs encoding for DCAF2. They were fixed at 12 h after microinjections (PN5 stage) and subjected to pH2AX immunofluorescence. Non-microinjected WT and $Dcaf2^{\text{♀}/\text{♂}^+}$ zygotes at the PB5 stage were used as negative and positive controls, respectively. Scale bar = 10 μm . **B:** Quantification of pH2AX foci in male and female pronucleus of WT and $Dcaf2^{\text{♀}/\text{♂}^+}$ zygotes at PN5. Error bars, s.e.m. *** $P < 0.001$ by two-tailed Student's t test.

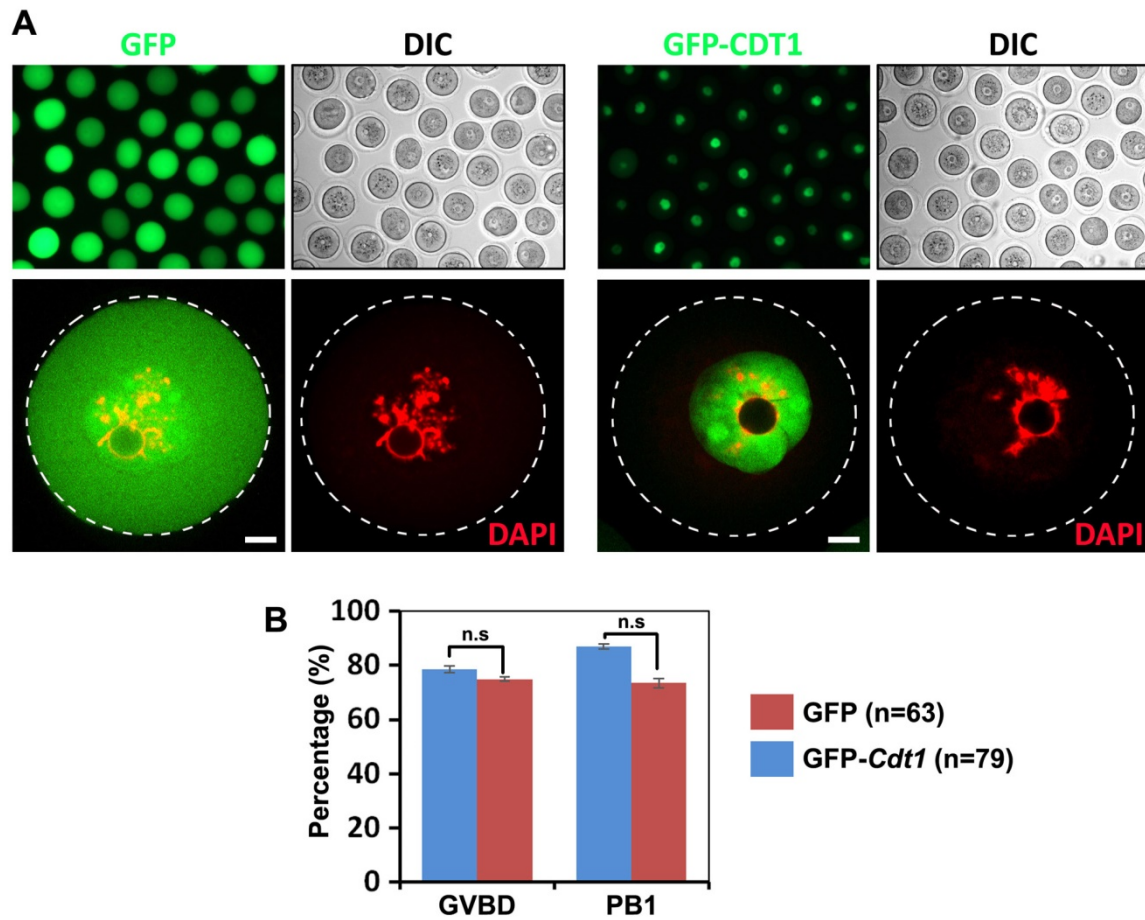


Figure S3: CDT1 overexpression in GV oocytes.

A: Localization of overexpressed GFP and GFP-CDT1 fusion proteins in GV oocytes after mRNA injections. Scale bar = 10 μ m. Error bars, S.E.M. n.s., not significant. **B:** GVBD and PB1 emission rates of oocytes overexpressing GFP or GFP-CDT1. n.s: non-significant.

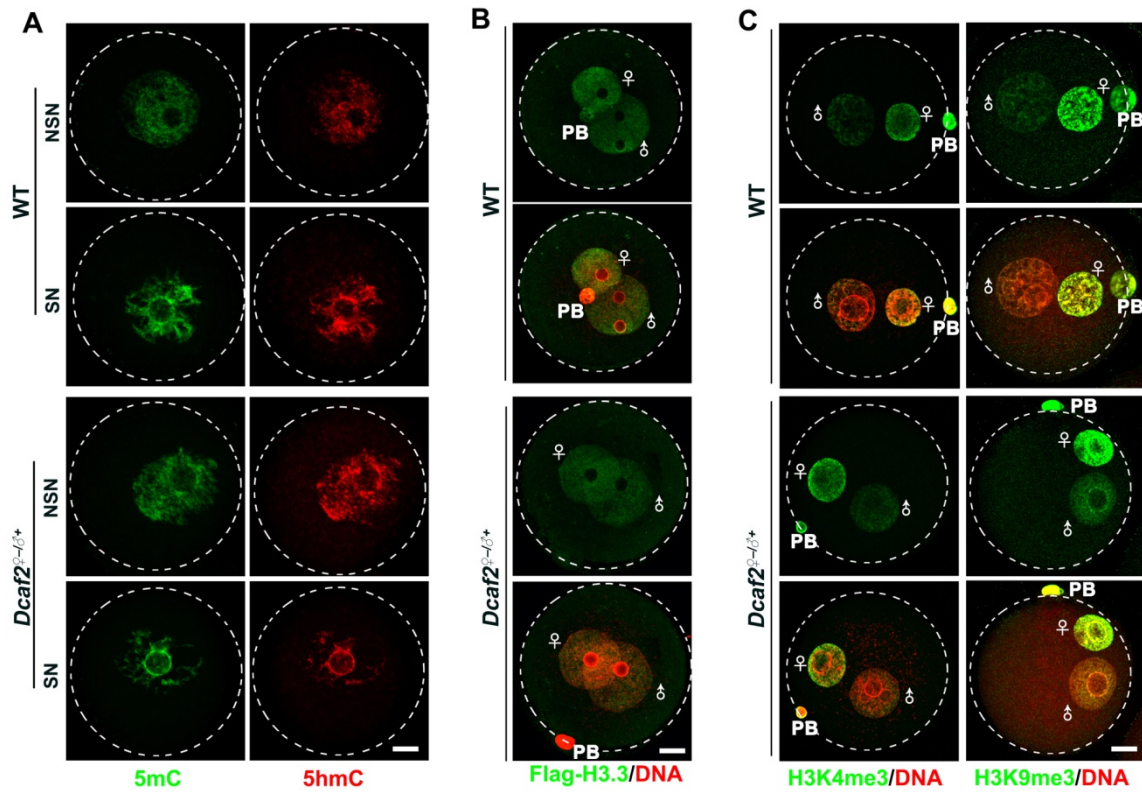


Figure S4: Levels of DNA and histone modifications in oocytes and zygotes of WT and *Dcaf2^{fl/fl};Gdf9-Cre* mice.

A: Immunofluorescence results showing DNA 5mC and 5hmC levels in oocytes of WT and *Dcaf2^{fl/fl};Gdf9-Cre* mice. NSN: non-surrounded nucleolus; SN: surrounded nucleolus. **B:** Immunofluorescence results showing trimethylation of histone H3 at lysine-4 (H3K4me3) and lysine-9 (H3K9me3). Scale bar = 10 μm.

Supplementary Table 1. Primer sequences.

Primer name	Genes targeted	Application	Sequences (5'-3')
FRT-F	<i>Dcaf2</i>	Identification of <i>Dcaf2</i> flox	5'- CAGTGGCCTTGTGCATACTA-3'
FRT-R			5'- GTTACACCTGGTGTCCCAGATC-3'
<i>iCre</i> -F	<i>Cre</i>	Identification of <i>Gdf9-Cre</i>	5'- GTGCAAGCTGAACAACAGGA-3'
<i>iCre</i> -R			5'- AGGGACACAGCATTGGAGTC-3'
<i>Dcaf2</i> -RT-F	<i>Dcaf2</i>	Real-time PCR (248 bp)	5'- AACCAGGTGATAAACATTCATAGTGGGTT-3'
<i>Dcaf2</i> -RT-R			5'- GACTGAAGAACGGGTCGTGGCAG-3'
<i>Cdt1</i> -RT-F	<i>Cdt1</i>	Real-time PCR (245 bp)	5'-TGGAGAAGGCCCTGAGCAACC-3'
<i>Cdt1</i> -RT-R			5'-CTCTGGCAGACGCTCTAACC GC-3'

Supplementary Table 2. Antibody information.

Protein name	Manufacture (catalogue number)	Applications (working dilution)	Website Link
H3K4me3	Abcam (ab8580)	IF (1:400)	http://www.abcam.com/histone-h3-tri-methyl-k4-antibody-chip-grade-ab8580.html
H3K9me3	Abcam (ab8898)	IF (1:400)	http://www.abcam.com/Histone-H3-tri-methyl-K9-antibody-ChIP-Grade-ab8898.html
FITC-α-Tubulin	Sigma (F2168)	IF (1:500)	http://www.sigmaaldrich.com/catalog/product/sigma/f2168?lang=zh&region=CN
BrdU	Sigma (B2531)	IF (1:500)	http://www.sigmaaldrich.com/catalog/product/sigma/b2531?lang=zh&region=CN
pH2AX (Ser139)	Cell Signaling (9718S)	IF (1:400)	http://www.cellsignal.com/products/primary-antibodies/phospho-histone-h2a-x-ser139-20e3-rabbit-mab/9718
5mC	Calbiochem (NA81)	IF (1:400)	http://www.merckmillipore.com/CN/zh/product/Anti-5-Methylcytosine-Mouse-mAb-%28162-33-D3%29,EMD_BIO-NA81?bd=1
5hmC	Active motif (39769)	IF (1:400)	https://www.activemotif.com/catalog/details/39769/5-hydroxymethylcytosine-5-hmc-antibody
RPA2	Gifted by Dr. Jun Huang	IF (1:50)	
CDT1	Santa Cruz (sc-28262)	IF (1:50)	http://www.scbt.com/datasheet-28262-cdt1-h-300-antibody.html
TET3	Gifted by Dr. Guoliang Xu	IF (1:50)	(Gu et al., 2011)

Reference

Gu, T. P., Guo, F., Yang, H., Wu, H. P., Xu, G. F., Liu, W., Xie, Z. G., Shi, L., He, X., Jin, S. G., et al. (2011). The role of Tet3 DNA dioxygenase in epigenetic reprogramming by oocytes. *Nature* **477**, 606-610.